

# Digital transmission using multimode phase-continuous chirp signals

K.R.Raveendra

Indexing terms: Digital transmission, Multimode phase-continuous chirp signals

**Abstract:** The concept of varying the modulation index of a continuous phase FSK (i.e. CPFSK) waveform is applied to digital transmission using chirp signals. These multimode chirp waveforms are described and their ability to perform over the coherent Gaussian channel is examined. It is shown that the dual-mode phase-continuous chirp signals out perform monomode signals by nearly 0.8dB, when corresponding high-SNR 5-bit optimum minimum-bit-error-probability receivers are employed. A low-complexity suboptimum average matched filter receiver for multimode chirp signals is examined and explicit expressions for its performance are given.

## 1 Introduction

In a spread-spectrum system the transmitted signal is spread over a wide frequency band, often much wider than the minimum bandwidth needed for the information to be conveyed. An instance of spectrum spreading may be seen in conventional FM by employing frequency deviations greater than unity. The wideband FM thus produced is often classified as a spread spectrum system because the radio frequency spectrum generated is much wider than that of the transmitted information. While in FM, the transmission bandwidth is a function of both information bandwidth and the amount of modulation, there exist techniques in which spectrum spreading is accomplished using some signal or operation other than the information signal that is transmitted. Besides direct-sequence modulation and FH/FSK, one technique is linear FM or chirp modulation [1] in which a carrier is swept over a wide band during a given data pulse interval.

Chirp modulation does not necessarily employ coding and produces a transmitted bandwidth much greater than the bandwidth of the information being sent. Furthermore, the growing interest in chirp systems is mainly due to the current state of art in surface acoustic wave (SAW) technology, which offers a rapid close-to-optimum way for both generation and correlation of wideband chirp pulses [2]. While chirp signals

have found their main application in radar systems [3], they were first proposed by Winkler [4], motivated by their anti-interference capability, for binary data communication. Further, chirp signals are useful in certain communication systems for reasons such as anti-eavesdrop, low-Doppler sensitivity etc. [1]. Among the several applications for binary chirp signals are air-ground communication via satellite repeaters [5, 6] and high frequency (HF) data transmission [7]. Combining the chirp signalling technique with some kind of pseudorandom coding, it is possible to achieve substantial improvement in antijam performance [8]. In [9], a spread spectrum transmission of digital data suggests a combination of chirp modulation and pseudonoise PSK.

The performances of coherent and noncoherent binary chirp signals over Gaussian channels have been studied in [10, 11]. The optimum receivers are required to make independent bit-by-bit decisions. Introducing phase continuity in chirp signal at bit transitions, allows for multiple bit detection schemes. These have been studied in [12, 13], where an advantage of at most 1.66dB over BPSK is demonstrated. While in these continuous phase chirp systems, the set of modulation parameters employed over any bit interval is the same, it is well known [14] that in a Continuous Phase FSK waveform by using time-varying modulation parameters, impressive gains in power are possible. It is the purpose of the paper to apply this concept to chirp signals. The resulting class of signals will be known as multimode continuous phase chirp modulation. Our results mainly include determination of optimum sets of modulation parameters over appropriate ranges and performance comparisons of the optimised signals with monomode continuous phase chirp signals, chirp signals with discontinuous phase and PSK.

## 2 Signal description and properties

Any digitally modulated continuous phase signal is represented as

$$S(t, \tilde{a}) = \sqrt{2E_b/T} \cos(2\pi f_c t + \phi(t, \tilde{a}) + \phi_0), \quad 0 \leq t \leq nT \quad (1)$$

where  $\tilde{a} = (a_1, a_2, \dots, a_n)$  is an  $n$ -bit uncorrelated equally likely binary sequence,  $E_b$  is the energy of the signal in the bit duration  $T$ ,  $f_c$  is the carrier frequency and  $\phi_0$  is the starting phase assumed to be zero for coherent transmission, and the information carrying phase is given by:

$$\phi(t, \tilde{a}) = \int_0^t \sum_{i=1}^n 2\pi a_i f(\tau - (i-1)T) d\tau \quad 0 \leq t \leq nT \quad (2)$$

© IEE, 1996

IEE Proceedings online no. 19960250

Paper first received 13th October 1994 and in revised form 29th August 1995

The author is with the Communication & Signal Processing Laboratory, Division of Electronics & Communication Engineering, Delhi Institute of Technology, Kashmere Gate, Delhi 110 006, India

where  $f(t)$  is the instantaneous frequency deviation during the  $i$ th bit interval and for multimode continuous phase chirp signalling is given by:

$$f(t) = \begin{cases} 0 & t \leq (i-1)T, t > iT \\ \frac{h_i}{2T} - \frac{w_i}{T^2}t & (i-1)T \leq t \leq iT \end{cases} \quad (3)$$

Representing the baseband phase function by:

$$g(t) = 2\pi \int_0^t f(\tau) d\tau \quad 0 \leq t \leq nT \quad (4)$$

eqn. 2 can be written as

$$\phi(t, \tilde{a}) = \sum_{i=1}^n a_i g(t - (i-1)T) \quad 0 \leq t \leq nT \quad (5)$$

where

$$g(t) = \begin{cases} 0 & t \leq (i-1)T, t > iT \\ \pi \left[ h_i \frac{t}{T} - w_i \left( \frac{t}{T} \right)^2 \right] & (i-1)T \leq t \leq iT \\ \pi q_i = \pi(h_i - w_i) & t = iT \end{cases} \quad (6)$$

In eqns. 3 and 6,  $h_i$  and  $w_i$  represent peak-to-peak frequency deviation divided by bit rate and frequency sweep width divided by bit rate, respectively, during the  $i$ th bit interval. The excess phase accumulated due to and at the end of the  $i$ th bit interval is  $\pm\pi q_i$  depending upon  $a_i = \pm 1$ . We denote the signal modulation parameters employed during the  $i$ th bit interval by the set  $\{w_i, q_i\}$ .

While in conventional (monomode) continuous phase chirp transmission  $w_i = w$  and  $q_i = q$ , for  $i = 1, 2, \dots$ , in multimode transmission we cyclically select  $\{w_i, q_i\}$  from a set  $\Omega_K$  of  $K$  sets of modulation parameters, i.e.

$$\Omega_K = \{ \{w_1, q_1\}, \{w_2, q_2\}, \dots, \{w_K, q_K\} \} \quad (7)$$

such that

$$w_{i+K} = w_i \quad (8)$$

and

$$q_{i+K} = q_i \quad (9)$$

thereby conveying that the signal parameter set used in the  $(i+K)$ th bit interval is the same as that used in the  $i$ th bit interval. That is  $\{w_i, q_i\}$ ;  $i = 1, 2, \dots$ , forms a sequence of sets with period  $K$ .

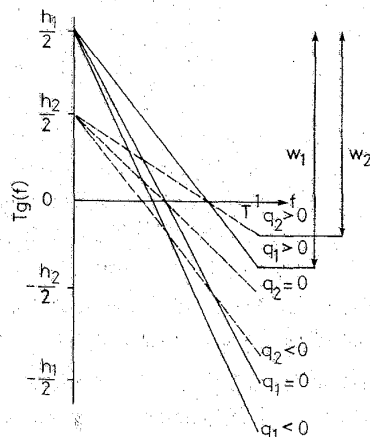


**Fig. 1** Instantaneous frequency deviations in dual-mode continuous phase chirp signalling system  
 $q_1 = h_1 - w_1$ ;  $q_2 = h_2 - w_2$

In Fig. 1, the instantaneous frequency deviations in a dual-mode continuous phase chirp signalling format is sketched. It is noted that this Figure illustrates the relations among the modulation parameters used during the  $i$ th bit interval (i.e.  $q_i = h_i - w_i$ ). In Fig. 2, all possible

phase evolutions of the phase function  $\phi(t) - \phi(0)$  are plotted for chirp system employing  $\{1.0, 0.25\}$ ,  $\{1.0, 0.5\}$ . Since the phase is modulo  $2\pi$ , this plot actually lies on the surface of a cylinder.

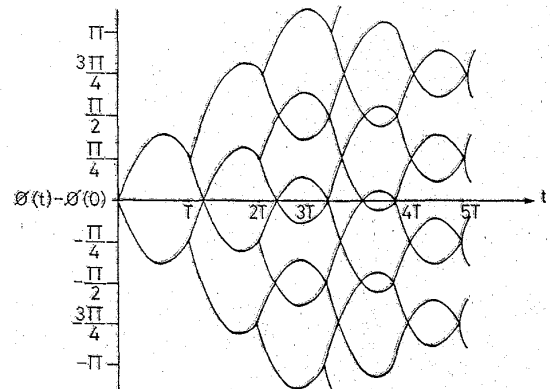


**Fig. 2** Phase trellis of binary dual-mode chirp signals with  $\Omega_2 = \{1.0, 0.25\}, \{1.0, 0.5\}$

By restricting the values  $q_i$  can assume to  $0 < q_i < 1$ , it is possible to apply, straightforwardly, the theory developed in [15] for multi- $h$  phase codes. Hence, by choosing  $q_i$ s from a set  $\{0 < q_i < 1; i = 1, 2, \dots, K\}$  such that  $q_i = 1/s$  ( $l_i$  and  $s$  being integers), it is possible to obtain a periodic phase trellis composed only of transitions between the  $2s$  values  $k\pi/s$  ( $k = 0, 1, \dots, 2s-1$ ). Further, if no two subsets of  $\{q_i\}$  have the same sum modulo one, a maximum constraint length for a given  $K$  is obtained. The set  $\{w_i\}$  may be chosen based on considerations such as spectral occupancy. Shown in Fig. 2 is the trellis structure with constraint length equal to 2 ( $=K$ ). This means that two trellis paths remain separated over at least 3 ( $=K+1$ ) bit intervals.

### 3 Receivers and performances

In this Section we briefly comment on the optimum and suboptimum receivers for multimode chirp signals and their performances in additive white Gaussian noise of one sided spectral density  $N_0$ . Ideal coherent detection is assumed.

The received signal may be written as [12, 16]:

$$r(t) = S^p(t, a_1, A_j) + n(t) \quad 0 \leq t \leq nT \quad (10)$$

where  $a_1$  is the first data bit and  $A_j$  is the  $(n-1)$ -tuple  $(a_2, a_3, \dots, a_n)$ ,  $n(t)$  is the additive white noise and the superfix  $p$  is used to denote the sequence of signal parameter sets  $(\{w_1, q_1\}, \dots, \{w_n, q_n\})$  in the received  $n$ -bit interval chirp signal. Following the development of [16], the optimum receiver that observes  $r(t)$  and produces an estimate  $\hat{a}_1$  of  $a_1$  is governed by the decision rule:

$$\sum_{j=1}^{2^{n-1}} \exp\left(\frac{2}{N_0} x_{\pm 1j}^p\right) \hat{a}_1 \geq \sum_{j=1}^{2^{n-1}} \exp\left(\frac{2}{N_0} x_{-1j}^p\right) \quad (11)$$

where

$$x_{\pm 1j}^p = \int_0^{nT} r(t) S^p(t, a_1 = \pm 1, A_j) dt \quad (12)$$

The receiver structure implied by eqn. 11 is identical to that employed for monomode chirp signals (Fig. 2; [12]), except that the receiver for multimode chirp signals has a priori information of the sequence of

signal parameter sets employed at the transmitter. While it is too complex to evaluate the performance of optimum receiver precisely, bounds tight at low and high SNRs can be determined.

For a large SNR approximation in eqn. 11, a suboptimum receiver is obtained that computes all  $x_{ij}^2$  and decides  $\hat{a}_1 = +1$  or  $-1$  accordingly as whether the largest one is within the set  $\{x_{+1j}^2\}$  or within the set  $\{x_{-1j}^2\}$ . The performance of this receiver may be upper and lower bounded using the union bounding technique [17]. The upper bound may be shown to be given by:

$$P_{e,\text{high SNR}} \leq \frac{1}{K} \frac{1}{2^{n-1}} \sum_{p=1}^K \sum_{l=1}^{2^{n-1}} \sum_{j=1}^{2^{n-1}} Q \left[ \left\{ \frac{nE_b}{N_0} (1 - \rho_p(l, j)) \right\}^{\frac{1}{2}} \right] \quad (13)$$

where  $\rho_p(l, j)$  is the normalised correlation between the transmitted signals  $S^p(t, a_1 = +1, A_j)$  and  $S^p(t, a_1 = -1, A_j)$ . A simple expression for this correlation for multi-mode chirp signals is given in the Appendix.

A lower bound on the performance of the high-SNR suboptimum receiver can be shown to be given by [16]:

$$P_{e,\text{high SNR}} > \frac{1}{K} \frac{1}{2^{n-1}} \sum_{p=1}^K \sum_{l=1}^{2^{n-1}} Q \left[ \left\{ \frac{nE_b}{N_0} (1 - \rho_p^*(l)) \right\}^{\frac{1}{2}} \right] \quad (14)$$

where  $\rho_p^*(l) = \max_j \rho_p(l, j)$ . Using eqns. 13 and 14, the error probability performance of the optimum receiver at large values of SNR can be estimated.

By using a low SNR approximation in eqn. 11 a suboptimum receiver that, for its operation, requires only two correlators is obtained. In the literature, this type of receiver is referred to as the average matched filter (AMF) receiver [18]. The performance of this receiver will provide an upper bound on the performance of the optimum receiver at low values of SNR, as the true performance of the optimum receiver is always better than that of the suboptimum receiver. The AMF receiver is governed by the decision rule:

$$r_p = \int_0^{nT} r(t) [\bar{s}^p(t, a_1 = +1) - \bar{s}^p(t, a_1 = -1)] dt \begin{matrix} \hat{a}_1 = +1 \\ > 0 \\ \hat{a}_1 = -1 \end{matrix} \quad (15)$$

where

$$\bar{s}^p(t, a_1 = \pm 1) = \sum_{j=1}^{2^{n-1}} S^p(t, a_1 = \pm 1, A_j) \quad (16)$$

The performance of the receiver given by eqn. 15 may be shown to be given by:

$$P_{e,\text{low SNR}} = \frac{1}{K} \frac{1}{2^{n-1}} \sum_{p=1}^K \sum_{j=1}^{2^{n-1}} Q \left[ \sqrt{\frac{E_b}{N_0} \frac{\mu_{+1j}^p}{\sigma_p^2}} \right] \quad (17)$$

where  $\mu_{+1j}^p$  is the expected value of the decision variable  $r_p$  given a particular data sequence  $A_j$  and  $a_1 = +1$  is transmitted and  $\sigma_p^2$  is the variance of  $r_p$ . For multi-mode chirp signalling closed-form expressions for  $\mu$  and  $\sigma$  are obtained and are given in the Appendix.

In eqns. 13, 14 and 17,  $Q[y]$  is the area under zero-mean unit-variance normal curve from  $y$  to  $\infty$ . Further, in these eqns.  $\Sigma_p$  has been used for averaging over all possible sequences of  $(\{w_1, q_1\}, \{w_2, q_2\}, \dots, \{w_n, q_n\})$ . While these eqns. may be used to evaluate bounds on the performance of the optimum receiver, a composite bound [16] that is representative of the true performance of the optimum receiver at all SNRs may be constructed by choosing the minimum of the high and low SNR upper bounds at all SNRs.

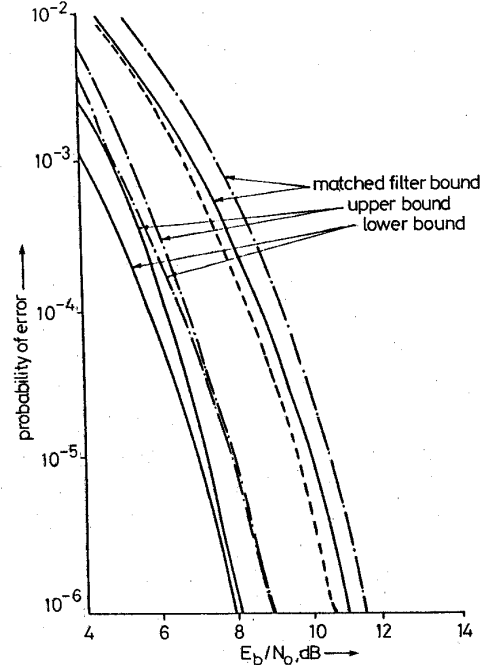


**Fig. 3** Performance of optimum  $\{(1.68, 0.27), (1.68, 0.49)\}$  dual-mode chirp set  $n = 4$   
 - - - - PSK  
 ———  $\{(1.68, 0.27), (1.68, 0.49)\}$   
 - · - · single mode,  $w = 2.33, q = 0.21$

#### 4 Numerical results

The performance bounds given by eqns. 13, 14 and 17 have been numerically computed for various cases. It is noted that the optimum receiver performance is a function of: i) SNR,  $E_b/N_0$ ; ii) number of observed bit intervals  $n$ ; iii) signal parameter set  $\Omega_K$ . For the case of  $K = 2$ , i.e. dual-mode binary chirp signals, sets  $\Omega_2 = \{\{w_1, q_1\}, \{w_2, q_2\}\}$  have been determined that minimise the performance bound of eqn. 13 for  $2 \leq n \leq 5$  and for SNR = 6, 8, 10dB. The minimisation has been carried out in the signal parameter space given by  $0 \leq w \leq 10 \times 0 \leq q_1, q_2 \leq 1$ , and the results are given in Table 1. The performance of the optimum receiver, in terms of lower and upper union bounds and the matched filter upper bound, for the optimum sets evaluated at an SNR of 8dB are shown in Figs. 3 and 4, for  $n = 4$  and  $n = 5$ ,

**Table 1. Optimum dual-mode continuous phase chirp sets**

$E_b/N_0$	$n = 2$	$n = 3$	$n = 4$	$n = 5$
6	{1.85; 0.28, 0.28}	{1.37; 0.26, 0.49}	{1.62; 0.27, 0.49}	{1.63; 0.30, 0.49}
8	{1.88; 0.27, 0.27}	{1.36; 0.26, 0.49}	{1.68; 0.27, 0.49}	{1.68, 0.30, 0.50}
10	{1.93; 0.26, 0.26}	{1.35, 0.26, 0.49}	{1.66; 0.28, 0.50}	{1.58; 0.31, 0.50}

{ $w, q_1, q_2$ } is used to denote  $\Omega_2 = \{(w, q_1), (w, q_2)\}$

respectively. In Fig. 5 is shown the performance upper bounds of the optimum monomode continuous and discontinuous phase chirp signals and the performances of dual-mode continuous phase chirp signals and PSK.

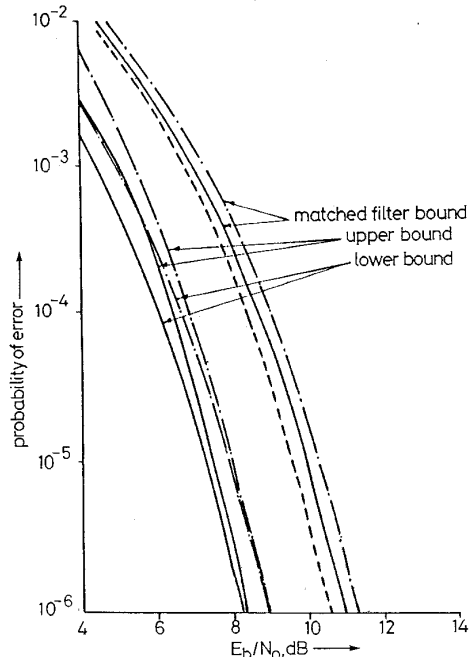


**Fig. 4** Performance of optimum  $\{\{1.68, 0.30\}, \{1.68, 0.50\}\}$  dual-mode chirp set  $n = 5$   
 --- PSK  
 —  $\{1.68, 0.3\}, \{1.68, 0.5\}$   
 -.- single mode,  $w = 2.37, q = 0.19$

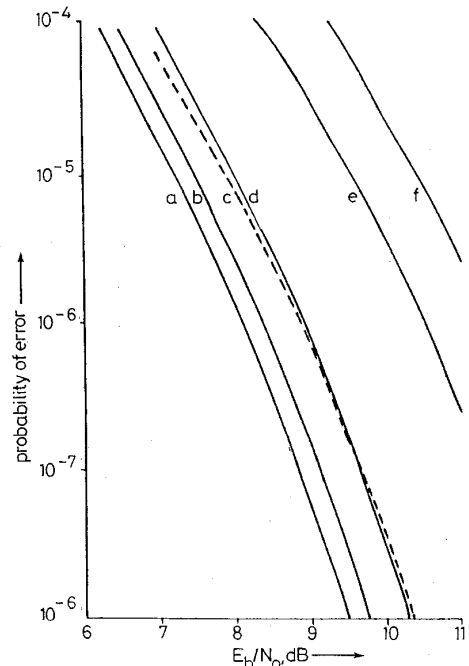


**Fig. 5** Performance comparison of optimum dual-mode chirp sets  
 a  $n = 5 \{1.68, 0.3\}, \{1.68, 0.50\}$   
 b  $n = 4 \{1.68, 0.27\}, \{1.68, 0.49\}$   
 c  $n = 5$  single mode,  $w = 2.37, q = 0.19$   
 d  $n = 3, \{1.36, 0.26\}, \{1.36, 0.49\}$   
 e PSK  
 f Single-bit optimum chirp signal

The optimised average matched filter receiver for dual-mode chirp signals provides a performance equal

to that of binary PSK. The performance is achieved for the optimum set  $\Omega_2 = \{\{w, 0.5\}, \{w, 0.5\}\}$  and an observation length of  $2T$ . In [12], it is shown that for monomode continuous phase chirp signals, the optimum matched filter performance occurs for  $\Omega_1 = \{w, 0.5\}$  and  $n = 2$ . These results can easily be verified analytically by examining equations given in the appendix for the performance of AMF receiver for multimode chirp signals. It can be shown that for dual-mode chirp signals the set  $\Omega_K = \{\{w, 0.5\}, \{w, 0.5\}\}$  provides performance equal to that of PSK for  $n = 2, 3, \dots$

From Table 1 we observe that, for a given  $n$ , the signal parameters of the optimum sets show mild variation with received SNR. Also, for dual-mode signals ( $K = 2$ ) it is noted that for  $n = 2$ , the optimum sets are with  $q_1 = q_2$  [12]. From Fig. 5, we observe that dual-mode chirp signals exist which are superior to binary PSK by 1.63, 2.15, and 2.40 dB for observation lengths  $3T, 4T$ , and  $5T$ , respectively. The optimum 3-bit dual-mode chirp system  $\{\{1.36, 0.26\}, \{1.36, 0.49\}\}$  performs nearly as well as the optimum 5-bit monomode system  $\{2.37, 0.19\}$ . Finally we observe that the optimum 5-bit dual-mode chirp system  $\{\{1.68, 0.30\}, \{1.68, 0.50\}\}$  outperforms optimum coherent single-bit discontinuous chirp system  $\{1.55, 0.35\}$  by nearly 3.4 dB.

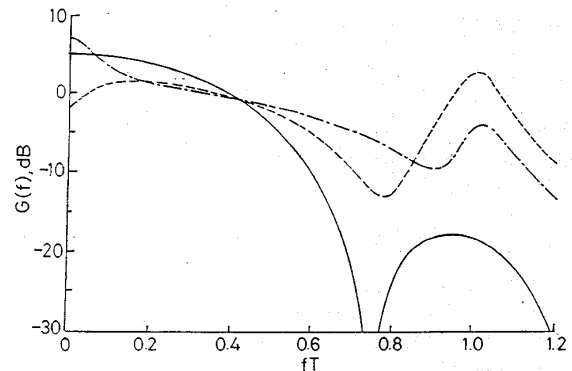


**Fig. 6** Power spectra of binary monomode chirp sets  
 — MSK  
 - - - ( $w = 1.55, q = 0.25$ )  
 -.- ( $w = 1.88, q = 0.27$ )

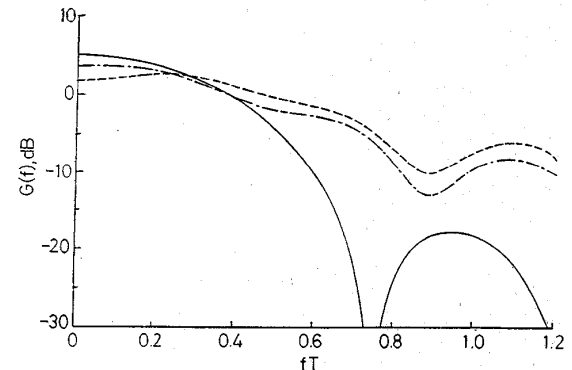


**Fig. 7** Power spectra of binary dual-mode chirp sets  
 — MSK  
 - - -  $\{1.68, 0.30\}, \{1.68, 0.50\}$   
 -.-  $\{1.36, 0.26\}, \{1.36, 0.50\}$

In Figs. 6 and 7 the normalised power spectra of monomode and dual-mode chirp systems have been plotted. In these Figures power spectrum of MSK are also given for comparison. It is noted from Fig. 6 that the difference between the maximum value of  $G(f)$  in

the main lobe and the maximum value in the first side lobe is nearly 11dB for  $\{w = 1.55, q = 0.25\}$  binary monomode chirp system and  $-1.4$ dB for  $\{w = 1.88, q = 0.27\}$  chirp system. This shows significant signal energy distribution in side lobes. The spectra of binary monomode chirp systems is quite sensitive to even small variations in the sweep width parameter  $w$ . It is noted that, as  $w$  increases, the ripple associated with spectra decreases, and as  $q$  ( $0 < q < 1$ ) increases, for a fixed  $w$ , the main lobe shifts away from frequency zero and the value of the peak itself increases in value.

## 5 Conclusions

In this paper we have introduced the concept of time-varying modulation parameters into the continuous phase chirp signals and analysed their performance ability over a coherent Gaussian channel. The optimum coherent receiver for multimode chirp signals is identified, for arbitrary observation intervals, and its error rate performance in terms of high and low SNR bounds have been determined. It has been shown that the dual-mode chirp system performs better than the known single-mode chirp system. A simple and easy-to-implement AMF receiver, for dual-mode chirp signals, has been obtained that performs close to that of the optimum receiver at low values of SNR. The best performance of this receiver is achieved with a minimum observation length of two bit intervals and for an unbounded range of  $w$  (the sweep width parameter of the signal), with  $q_1 = q_2 = 0.5$ . The performance thus achieved is equal to that of PSK.

Although the numerical results presented in this paper are for dual-mode chirp systems, our treatment of the problem and analytical results presented, in general, hold good for arbitrary multimode chirp systems.

## 6 Acknowledgment

The author wishes to thank the anonymous referees for their many helpful suggestions on presenting the material.

## 7 References

- DIXON, R.C.: 'Spread spectrum systems' (Wiley, New York, 1976)
- MATTHEWS, H. (Ed.): 'Surface wave filters: design, construction and use' (Wiley, New York, 1977)
- KLAUDER, J.R., PRICE, A.C., DARLINGTON, S., and ALBERSHEIM, W.J.: 'The theory and design of chirp radars', *Bell Syst. Tech. J.*, 1960, xxxix, (4), pp. 745-808
- WINKLER, M.R.: 'Chirp signals for communications', IEEE WESCON Convention Record, 1962
- BARNES, G.W., HIRST, D., and JAMES, D.J.: 'Chirp modulation systems in aeronautical satellites', AGARD conference proceedings, No. 87 Avionics in spacecraft, Royal Aircraft Estb., Rome, Italy, 1971
- BURNSWEIG, J., and WOOLRIDGE, J.: 'Ranging and data transmission using digital encoded FM-chirp surface acoustic wave filters', *IEEE Trans.*, 1973, SU-20, pp. 190-197
- GOTT, G.F., and NEWSOME, J.P.: 'H. F. data transmission using chirp signals', *Proc. IEE*, 1971, 118, pp. 1162-1166
- BUSH, H., MARTIN, A.R., COBB, R.E., and YOUNG, E.: 'Applications of chirp SWD for spread spectrum communications', *Proc.*
- KOWATSCH, M., and LAFFERL, J.T.: 'A spread spectrum concept combining chirp modulation and pseudonoise coding', *IEEE Trans.*, 1983, COM-31, pp. 1131-1142
- BERNI, A.J., and GREGG, W.D.: 'On the utility of chirp modulation for digital signaling', *IEEE Trans.*, 1973, COM-21, pp. 748-751
- ZAYTSEV, D.L., and ZHURAVLEV, V.I.: 'Noise immunity of a digital data transmission system using linearly frequency modulated signals', *Telecommunications (USSR)*, 1968, 22, pp. 13-17

- HIRT, W., and PASUPATHY, S.: 'Continuous phase chirp (CPC) signals for binary data communication. Part I: coherent detection', *IEEE Trans.*, 1981, COM-29, pp. 836-847
- HIRT, W., and PASUPATHY, S.: 'Continuous phase chirp (CPC) signals for binary data communication. Part II: noncoherent detection', *IEEE Trans.*, 1981, COM-29, pp. 848-858
- TANAKA, Y., HARASHIMA, H., and MIYAKAWA, H.: 'Multi-mode binary CPFSS', *Electr. Commun., Japan*, 1975, 58-A, (11)
- ANDERSON, J.B., and TAYLOR, D.P.: 'A bandwidth efficient class of signal-space codes', *IEEE Trans.*, 1978, IT-24, pp. 703-712
- OSBORNE, W.P., and LUNTZ, M.B.: 'Coherent and noncoherent detection of CPFSS', *IEEE Trans.*, 1974, COM-22, pp. 1023-1036
- BHARGAVA, V.K., HACCOUN, D., MATYAS, R., and NUSPL, P.: 'Digital communications by satellite' (Wiley, New York, 1981), pp. 191-193
- PELCHAT, M.G., DAVIS, R.C., and LUNTZ, M.B.: 'Coherent demodulation of continuous phase binary FSK signals', Proceedings of the international Telemetry conference, Washington, DC, 1971, pp. 181-190
- RAVEENDRA, K.R., and SRINIVASAN, R.: 'Coherent detection of binary multi-h CPM', *IEE Proc. F*, 1987, 134, pp. 416-426
- ABROMOWITZ, M., and STEGUN, I.A.: 'Hand book of mathematical functions' (National Bureau Standards, Washington, DC, 1964)

## 8 Appendix

### 8.1 Correlation expression for multimode chirp signals

An expression for the normalised sequence correlation required in eqns. 13 and 14 may be shown to be given by:

$$\rho_p(i, j) = \frac{1}{n} \sum_{k=1}^n \rho_{pk}(i, j) \quad (18)$$

where

$$\rho_{pk}(i, j) = \begin{cases} \cos(\pi \sum_{r=1}^{k-1} \gamma_r q_r^p) & \gamma_k = 0 \\ (2|\gamma_k|w_k^p)^{-\frac{1}{2}} \{\cos(\Theta_k^p) \Phi_k^p + \sin(\Theta_k^p) \Psi_k^p\} & \gamma_k \neq 0 \end{cases} \quad (19)$$

with

$$\Theta_k^p = \frac{0.25}{w_k^p} \pi |\gamma_k| (w_k^p - q_k^p)^2 + \text{sgn}(a_k^i - a_k^j) \pi \sum_{r=1}^{k-1} \gamma_r q_r^p \quad (20)$$

$$\Phi_k^p = C(\beta_-) + C(\beta_+) \quad (21)$$

$$\Psi_k^p = S(\beta_-) + S(\beta_+) \quad (22)$$

where

$$\gamma_k = a_k^i - a_k^j \quad (23)$$

and

$$\beta_{\pm} = (|\gamma_k|/2w_k^p)^{\frac{1}{2}} (w_k^p \pm q_k^p) \quad (24)$$

The terms  $a_k^i$  and  $a_k^j$  denote  $k$ th data bits of the  $i$ th and  $j$ th sequences with  $a_1^i = +1$  and  $a_1^j = -1$ . The parameters  $w_k^p$  and  $q_k^p$  belong to the  $k$ th set of  $p$ th of  $K$  possible sequences of sets  $\{w_1, q_1\}, \{w_2, q_2\}, \dots, \{w_n, q_n\}$  [19].

### 8.2 Closed-form expressions for $\mu$ and $\sigma$

The expressions for  $\mu$  and  $\sigma$  required in eqn. 17 are given by

$$\mu_{+1j}^p = M_1^p + \sum_{k=2}^n M_{jk}^p \quad (25)$$

and

$$\sigma_p^2 = V_1^p + \sum_{k=2}^n V_k^p \quad (26)$$

where

$$M_1^p = 1 - \frac{1}{\sqrt{w_1^p}} \{\cos(\Phi_1^p) \Lambda_1^p + \sin(\Phi_1^p) \Gamma_1^p\} \quad (27)$$

$$M_k^p = \sin(\pi q_k^p) \prod_{i=1}^k \cos^{\alpha_i(k)}(\pi q_i^p) \left\{ \sin(\theta_{jk}^p) + \frac{a_k^j}{2\sqrt{w_k^p}} [\sin(\Phi_k^p)\Lambda_k^p - \cos(\Phi_k^p)\Gamma_k^p] \right\} \quad (28)$$

$$V_k^p = 1 - \frac{1}{2\sqrt{w_1^p}} \{ \cos(\Theta_1^p)\Lambda_1^p + \sin(\Theta_1^p)\Gamma_1^p \} \quad (29)$$

and

$$V_k^p = 0.5(1 - \cos 2\pi q_1^p) \prod_{i=1}^k \cos^{2\alpha_i(k)}(\pi q_i^p) \left[ 1 + \frac{1}{2\sqrt{w_k^p}} \{ \cos(\Theta_k^p)\Lambda_k^p + \sin(\Theta_k^p)\Gamma_k^p \} \right] \quad (30)$$

with

$$\Phi_k^p = \frac{\pi}{2w_k^p} (w_k^p + q_k^p)^2 + \text{sgn}(a_k^j)\theta_{jk}^p \quad (31)$$

$$\Theta_k^p = \frac{\pi}{2w_k^p} (w_k^p + q_k^p)^2 \quad (32)$$

$$\Lambda_k^p = C(\nu_-) + C(\nu_+) \quad (33)$$

$$\Gamma_k^p = S(\nu_-) + S(\nu_+) \quad (34)$$

$$\theta_{jk}^p = \pi \sum_{r=1}^{k-1} a_r^j q_r^p \quad (35)$$

$$\nu_{\pm} = \frac{w_k^p \pm q_k^p}{\sqrt{w_k^p}} \quad (36)$$

In eqns. 28 and 30  $\alpha_i(\cdot)$  are as given in Table 1 of [19]. The functions  $C(\cdot)$  and  $S(\cdot)$  are the standard Fresnel integrals defined as [20]

$$C(x) = \int_0^x \cos \frac{\pi}{2} y^2 dy \quad (37)$$

and

$$S(x) = \int_0^x \sin \frac{\pi}{2} y^2 dy \quad (38)$$

In eqns. 28 and 35  $a_k^j$  refers to the  $k$ th data bit of the  $j$ th of the  $2^{n-1}$  data sequences that can be transmitted with the first bit data always equal to a +1.